



# ChestX-ray8: Hospital-scale Chest X-ray Database and Benchmarks on Weakly-Supervised Classification and Localization of Common Thorax Diseases

Xiaosong Wang<sup>1</sup>, Yifan Peng<sup>2</sup>, Le Lu<sup>1</sup>, Zhiyong Lu<sup>2</sup>, Mohammadhadi Bagheri<sup>1</sup>, Ronald M. Summers<sup>1</sup>

<sup>1</sup> Department of Radiology and Imaging Sciences, Clinical Center; <sup>2</sup> National Center for Biotechnology Information, National Library of Medicine

National Institutes of Health, Bethesda, MD 20892

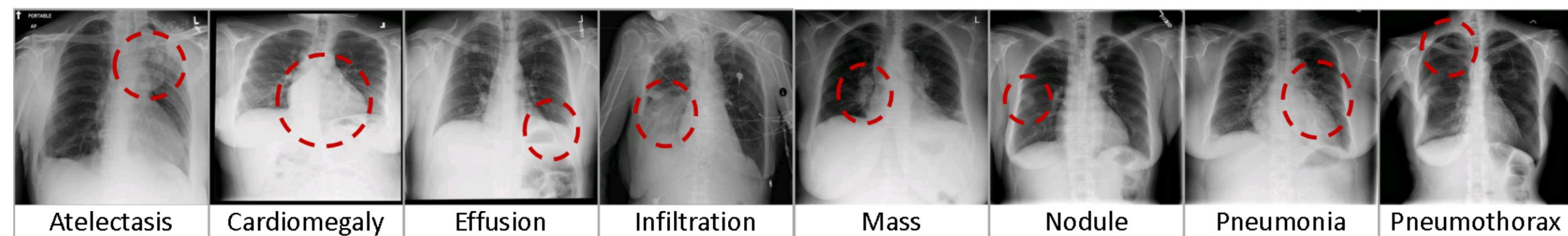


Scan to contact

## Highlights

- A new **Chest X-ray dataset** with 108,948 frontal view scans of 32,717 unique patients with the text mined disease image labels and meta info.
- A **weakly-supervised** multi-disease detection and localization framework

## Dataset Scope: Common Thorax Diseases



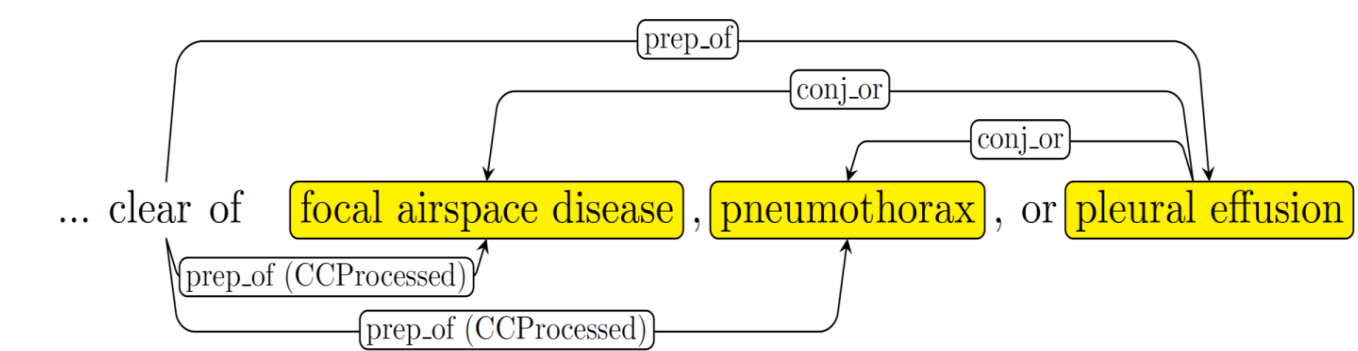
## 2-stage Disease Label Mining via NLP

### Stage 1: Pathology Detection

- DNorm and MetaMap is used to detect disease keywords in a report using either concept in SNOMED-CT or UMLS Metathesaurus

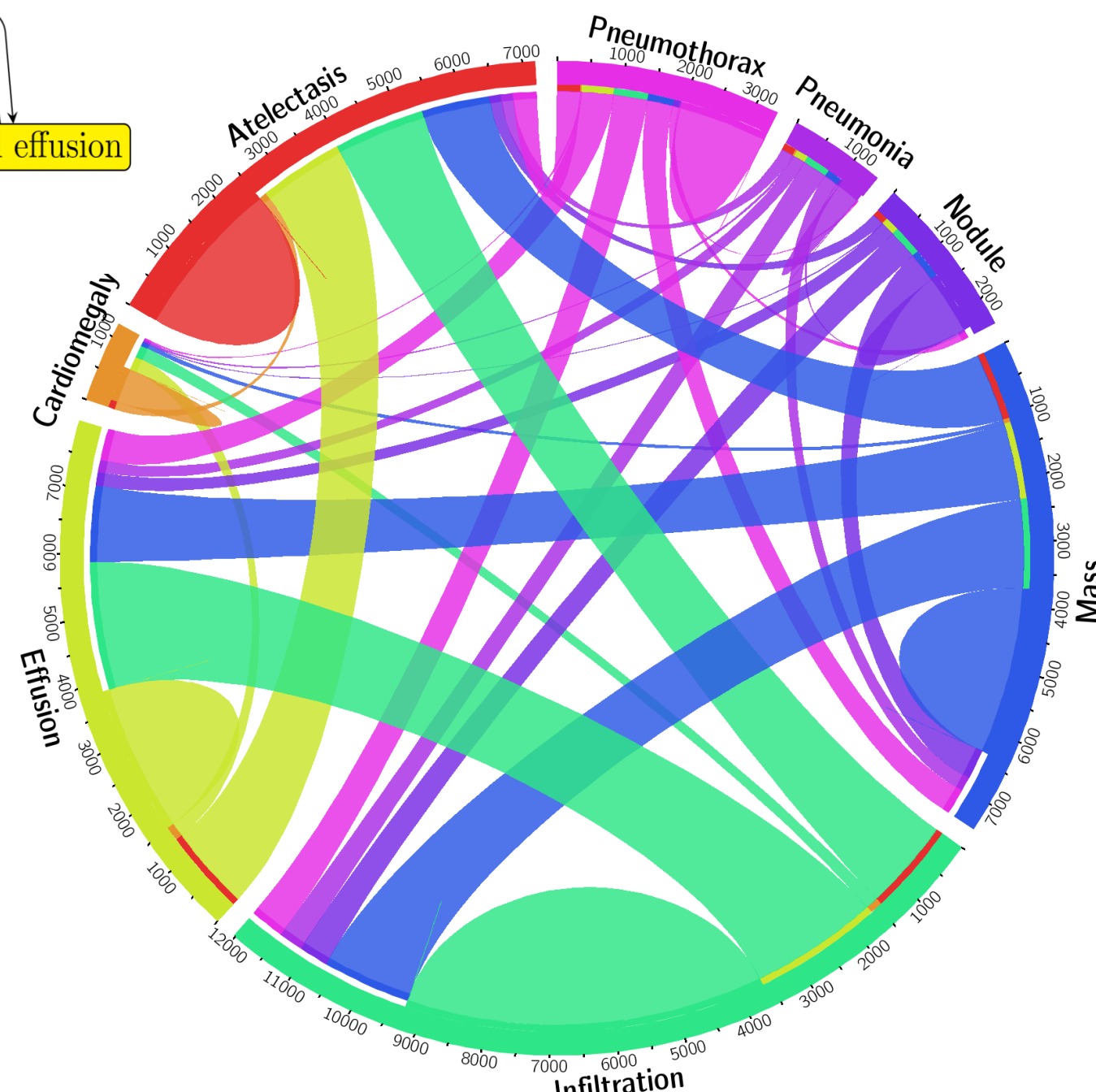
### Stage 2: Removal of negation and uncertainty

- Rule out those negated pathological statements and uncertain mentions of findings, e.g.  $\text{no} \leftarrow \text{neg} \leftarrow \text{evidence} \rightarrow \text{prep\_of} \rightarrow \text{DISEASE}$
- Defined the rules on the dependency graph, by utilizing the dependency label and direction information between words, e.g.



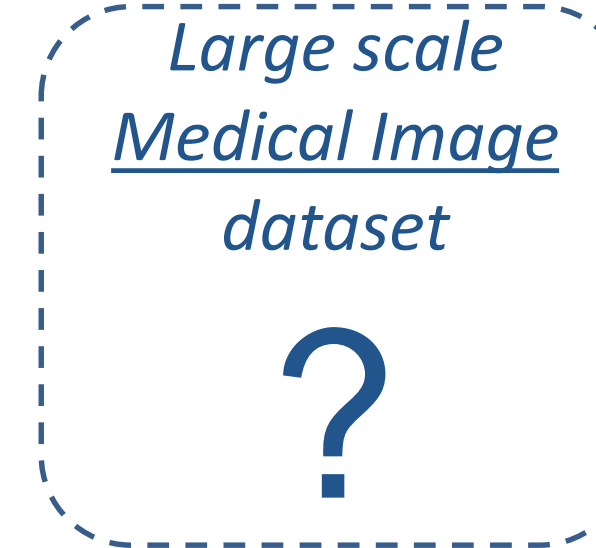
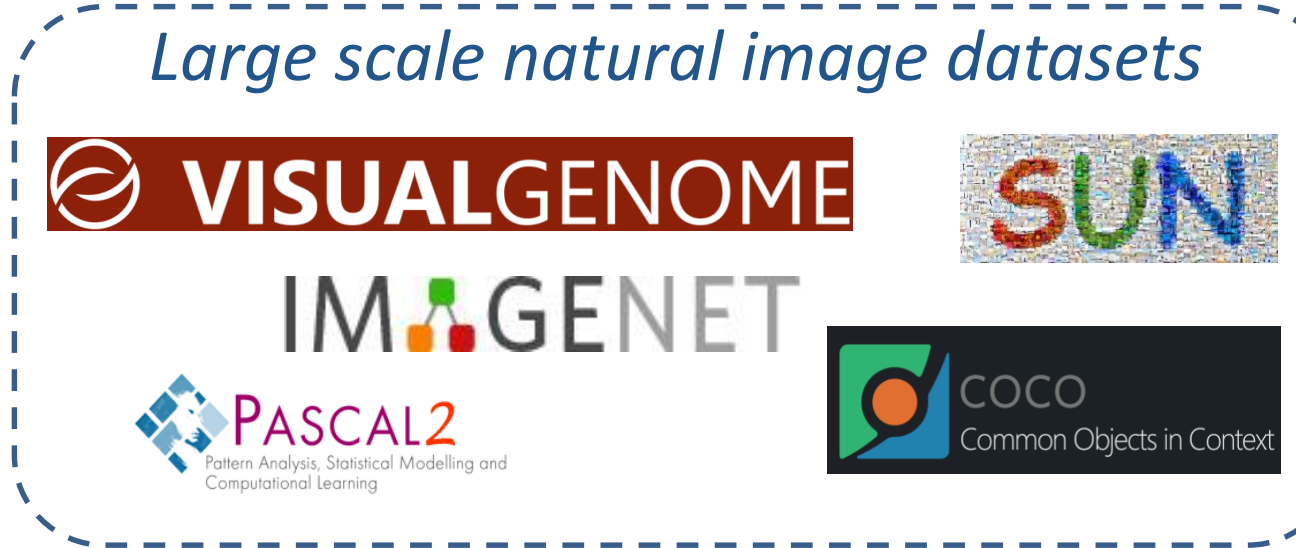
## Disease Category Statistics

| Item #       | OpenI | Ov. | ChestX-ray8 | Ov.   |
|--------------|-------|-----|-------------|-------|
| Report       | 2,435 | -   | 108,948     | -     |
| Annotations  | 2,435 | -   | -           | -     |
| Atelectasis  | 315   | 122 | 5,789       | 3,286 |
| Cardiomegaly | 345   | 100 | 1,010       | 475   |
| Effusion     | 153   | 94  | 6,331       | 4,017 |
| Infiltration | 60    | 45  | 10,317      | 4,698 |
| Mass         | 15    | 4   | 6,046       | 3,432 |
| Nodule       | 106   | 18  | 1,971       | 1,041 |
| Pneumonia    | 40    | 15  | 1,062       | 703   |
| Pneumothorax | 22    | 11  | 2,793       | 1,403 |
| Normal       | 1,379 | 0   | 84,312      | 0     |



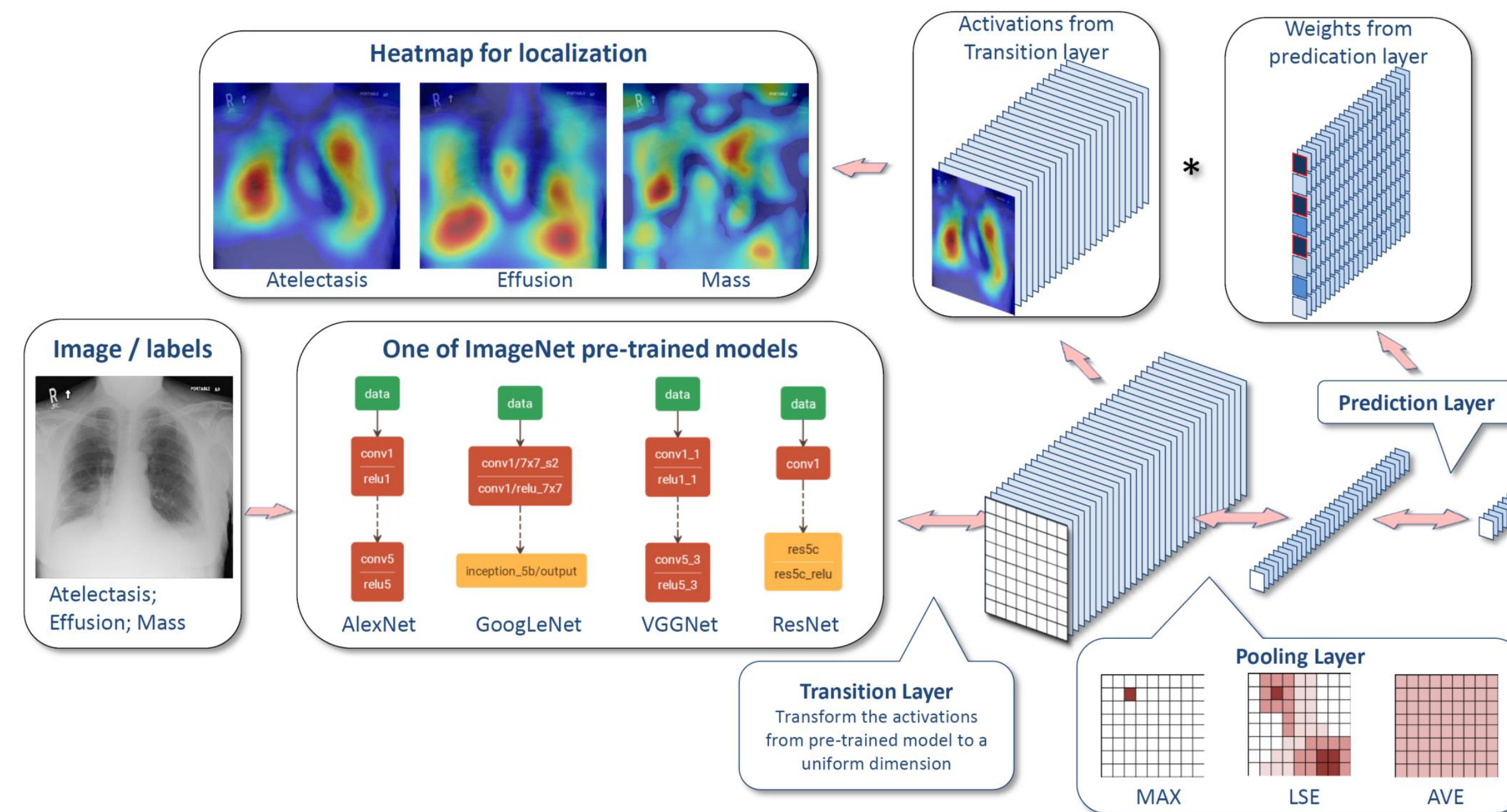
## Motivation

- Well-labeled data are the key for large scale machine learning paradigms and image labeling method, e.g. AMT are NOT applicable to medical images
- Detection and localization of all common thorax diseases in one go



## Multi-label Classification and Localization Framework

- Multi-label Setting:** 8-D disease label vector,  $[y_1, \dots, y_c, \dots, y_C], y_c \in \{0, 1\}, C = 8$



- Transition Layer:** Transform the activations from previous layers into a uniform dimension of output  $S \times S \times D, S \in \{8, 16, 32\}$
- Multi-label Classification Loss Layer:** positive/negative balancing, e.g.

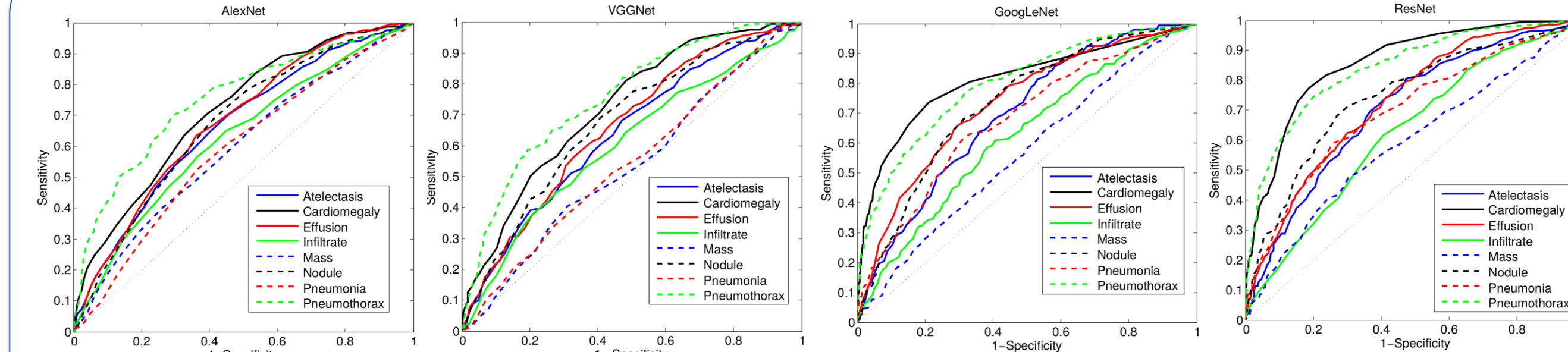
$$L_{W-CEL}(f(\vec{x}), \vec{y}) = \beta_P \sum_{y_c=1} -\ln(f(x_c)) + \beta_N \sum_{y_c=0} -\ln(1 - f(x_c)),$$

- Global Pooling Layer:** the Log-Sum-Exp (LSE) pooling, which is defined as

$$x_p = \frac{1}{r} \cdot \log \left[ \frac{1}{S} \cdot \sum_{(i,j) \in S} \exp(r \cdot x_{ij}) \right] \quad x_p = x^* + \frac{1}{r} \cdot \log \left[ \frac{1}{S} \cdot \sum_{(i,j) \in S} \exp(r \cdot (x_{ij} - x^*)) \right]$$

where  $x^* = \max\{x_{ij}, (i, j) \in S\}$ .

## Multi-disease Classification Results



| Setting  | Atelectasis   | Cardiomegaly  | Effusion      | Infiltration  | Mass          | Nodule        | Pneumonia     | Pneumothorax  |
|--|---------------|---------------|---------------|---------------|---------------|---------------|---------------|---------------|
| Initialization with different pre-trained models |               |               |               |               |               |               |               |               |
| AlexNet  | 0.6458        | 0.6925        | 0.6642        | 0.6041        | <b>0.5644</b> | 0.6487        | 0.5493        | 0.7425        |
| GoogLeNet  | 0.6307        | 0.7056        | 0.6876        | 0.6088        | 0.5363        | 0.5579        | 0.5990        | 0.7824        |
| VGGNet-16  | 0.6281        | 0.7084        | 0.6502        | 0.5896        | 0.5103        | 0.6556        | 0.5100        | 0.7516        |
| ResNet-50  | <b>0.7069</b> | <b>0.8141</b> | <b>0.7362</b> | <b>0.6128</b> | 0.5609        | <b>0.7164</b> | <b>0.6333</b> | <b>0.7891</b> |
| Different multi-label loss functions             |               |               |               |               |               |               |               |               |
| CEL  | 0.7064        | 0.7262        | 0.7351        | 0.6084        | 0.5530        | 0.6545        | 0.5164        | 0.7665        |
| W-CEL  | 0.7069        | 0.8141        | 0.7362        | 0.6128        | 0.5609        | 0.7164        | 0.6333        | 0.7891        |

Table 3. AUCs of ROC curves for multi-label classification in different DCNN model setting.

## Disease Localization Results

| T(IoBB)   | Atelectasis | Cardiomegaly | Effusion | Infiltration | Mass   | Nodule | Pneumonia | Pneumothorax |
|---|-------------|--------------|----------|--------------|--------|--------|-----------|--------------|
| <b>T(IoBB) = 0.25</b> (Two times larger on both x and y axis than ground truth B-Boxes) |             |              |          |              |        |        |           |              |
| Acc.  | 0.5500      | 0.9794       | 0.5424   | 0.5772       | 0.2823 | 0.0506 | 0.5583    | 0.3469       |
| AFP   | 0.1666      | 0.1534       | 0.1189   | 0.0914       | 0.0975 | 0.0741 | 0.1250    | 0.0487       |
| <b>T(IoU) = 0.5</b>   |             |              |          |              |        |        |           |              |
| Acc.  | 0.0500      | 0.1780       | 0.1111   | 0.0650       | 0.0117 | 0.0126 | 0.0333    | 0.0306       |
| AFP   | 0.3384      | 0.5335       | 0.2510   | 0.2408       | 0.1483 | 0.0772 | 0.2926    | 0.0965       |

| Radiology report  | Keyword          | Localization Result | Radiology report  | Keyword                 | Localization Result |
|---|------------------|---------------------|---|-------------------------|---------------------|
| findings: no appreciable change since XXXXX. small right pleural effusion. elevation right hemidiaphragm. diffuse small nodules throughout the lungs, most numerous in the left mid and lower lung. impression: no change with bilateral small lung metastases. | Effusion; Nodule |                     | findings: unchanged left lower lung field infiltrate/air bronchograms. unchanged right perihilar infiltrate with obscuration of the right heart border. no evidence of new infiltrate. no evidence of pneumothorax the cardiac and mediastinal contours are stable. impression: 1. no evidence pneumothorax. 2. unchanged left lower lobe and left lingular consolidation/bronchiectasis. 3. unchanged right middle lobe infiltrate | Pneumonia; Infiltration |                     |
| findings include: 1. cardiomegaly (ct ratio of 17/30). 2. otherwise normal lungs and mediastinal contours. 3. no evidence of focal bone lesion. dictating   | Cardiomegaly     |                     | findings: frontal lateral chest x-ray performed in expiration. left apical pneumothorax visible. small pneumothorax visible along the left heart border and left hemidiaphragm. pleural thickening. mass right chest. the mediastinum cannot be evaluated in the expiration. bony structures intact. impression: left post biopsy pneumothorax.   | Mass; Pneumothorax      |                     |



Download the NIH ChestX-ray dataset via Google Cloud

[https://console.cloud.google.com/storage/gcs-public-data-nih/radiology\\_2017/Chest\\_X-Ray\\_CVPR17/images](https://console.cloud.google.com/storage/gcs-public-data-nih/radiology_2017/Chest_X-Ray_CVPR17/images)

## Acknowledgement

- This work was supported by the Intramural Research Programs of the NIH Clinical Center and National Library of Medicine.
- We thank Nvidia corporation for the GPU donation.